

QUANTUM TECHNOLOGIES: The information revolution that will change the future





Analysis of the Impact of Homodyne Detection Efficiency on Remote State Preparation

Wagner C. Normando Filho*,1, Leonardo J. Pereira1, and Alexandre B. Tacla1

¹QuIIN - Quantum Industrial Innovation, EMBRAPII CIMATEC Competence Center in Quantum Technologies, SENAI CIMATEC, Av. Orlando Gomes 1845. 41650-010, Salvador, BA, Brazil

Abstract: Continuous-variable quantum key distribution (CV-QKD) is a leading technology for secure communication, whose security guarantees fundamentally rely on the quantum nature of the transmitted states and the measurement process. However, real-world detectors invariably suffer from limitations, such as inefficiency, which affects the overall security and performance of the system. Here, we investigate the impact of detector efficiency on remote state preparation in the context of entanglement-based CV-QKD. Specifically, by using the Wigner function formalism and starting from a two-mode squeezed vacuum state, we derive the analytical form of the quantum state of one mode conditioned on a homodyne measurement performed on the other mode. Our analysis explicitly contrasts the ideal case of unit efficiency (η =1), which prepares a pure, displaced squeezed state, with the non-ideal scenario. For $\eta < 1$, we demonstrate that the preparation result is a mixed state characterized by increased noise and degraded squeezing. We calculate the exact analytical expressions for the conditional state's variance and mean displacement, quantifying their dependence on both the efficiency η and the initial squeezing parameter.

Keywords: Wigner function, efficiency detection, noise detector

Abbreviations: Continous-variable quantum key distribution, CV-QKD; discrete-variable quantum key distribution, CV-QKD; Einstein-Podolsky-Rosen, EPR; Frédéric Grosshans and Philippe Grangier 2002, GG02

1. Introduction

Continuous-variable quantum key distribution (CV-QKD) represents one of the most promising approaches in secure quantum communication. Unlike discrete-variable QKD, CV-QKD encodes information in the quadratures of electromagnetic fields. This approach offers significant advantages, such as compatibility with standard telecommunication components, potentially high secret key rates and straightforward integration with existing optical fiber infrastructures [1, 2].

In entanglement-based CV-QKD, the protocol begins with the sender, Alice, generating pairs of entangled continuous-variable states, typically two-mode squeezed vacuum states. She then keeps one mode to herself and sends the other mode to the receiver, Bob. Both parties independently per-

form quadrature measurements (homodyne or heterodyne detection) on their respective entangled modes, obtaining correlated measurement results. After this quantum phase, Alice and Bob perform standard post-processing procedures to extract a symmetric secure secret key: they perform parameter estimation, then apply error correction and privacy amplification. Generally, the security and performance of this protocol is affected by the detector's noise and efficiency [1, 3].

In this work, we investigate theoretically the impact of Alice's homodyne detection efficiency on the remote preparation of Bob's state. Theoretically, such a detector can be modeled by placing a beam splitter with transmittance η before the homodyne detector [4, 5, 6, 7, 8]. For this purpose, we employ the phase-space formalism of the Wigner function, a powerful tool that pro-

ISSN: 2357-7592







vides a quasi-probabilistic and intuitive representation of quantum states [9]. We start from a twomode squeezed vacuum state, a fundamental resource for generating continuous-variable entanglement. We analyze the quantum state of Bob's mode b conditioned on the outcome of a homodyne measurement performed on Alice's mode a. By calculating and visualizing the Wigner function of the conditioned state in mode b, we graphically demonstrate how measurement inefficiency modify properties of the state, such as its degree of squeezing. In the ideal case of unit efficiency $(\eta=1)$, Alice projects Bob's state into a pure, displaced squeezed state. For $\eta < 1$, we show that the preparation result is a mixed state characterized by increased noise and degraded squeezing.

2. Wigner function formalism

The Wigner function, W(x,p), is the main tool of the phase-space formalism. It is a quasi-probability function that maps the density operator of a quantum state, $\hat{\rho}$, onto a real function in the classical phase space defined by the variables (x,p). In the one-dimensional case, it is defined as the Fourier transform of the displaced density operator in the position representation [10, 9]:

$$W_{\hat{\rho}}(x,p) = \frac{1}{2\pi\hbar} \int e^{-\frac{ipy}{\hbar}} \langle x - \frac{y}{2} | \hat{\rho} | x + \frac{y}{2} \rangle dy \quad (1)$$

This equation maps the density matrix, defined in Hilbert space, to a function in the one-dimensional phase space, thus providing an equivalent way of describing the quantum state of the physical system under study [11, 8, 9]. The Wigner function formalism is complete in the sense that it reproduces all quantum-mechanical results obtained through the traditional Hilbert-space approach. [11]

Just as in the traditional formalism, where measurements are described by Hermitian operators, the phase-space formalism also allows such operators to be represented by functions in phase space. This mapping from operators to functions is formally known as the *Weyl symbol* and is defined as [12]:

$$W_{\hat{A}}(x,p) = \int e^{-\frac{ipy}{\hbar}} \langle x - \frac{y}{2} | \hat{A} | x + \frac{y}{2} \rangle dy, \quad (2)$$

where \hat{A} is an arbitrary operator.

Equations Eq. 1 and Eq. 2 are structurally very similar. The first includes a constant factor ensuring normalization, as physically realizable states must be normalized.

If \hat{A} is Hermitian, the result of Eq. 2 is a real-valued function in phase space [12]. In the literature, the Weyl symbol is also commonly referred to as the *Wigner function of an operator*. Notably, the Wigner function in 1 is simply the Weyl symbol of the density operator $\hat{\rho}$, multiplied by the factor $\frac{1}{2\pi\hbar}$.

QUANTUM TECHNOLOGIES: The information revolution that will change the future





3. Ideal vs non-ideal homodyne detection

The two-mode squeezed vacuum state (EPR state) can be expressed in the Fock basis as follows [8]:

$$|\psi_{sq}\rangle_{ab} = (1-\lambda^2)^{1/2} \sum_{n=0}^{\infty} \lambda^n |n\rangle_a \otimes |n\rangle_b.$$
 (3)

Where $\lambda = tanh(\zeta)$ with ζ being the squeezing parameter. In the Wigner function formalism, the EPR state above is expressed as [8]:

$$W(a,b) = Ke^{-\frac{(x_a - x_b)^2}{4\sigma_0 s^2} - \frac{(x_a + x_b)^2}{4\sigma_0^2/s} - \frac{(p_a - p_b)^2}{4\sigma_0^2/s} - \frac{(p_a + p_b)^2}{4\sigma_0^2 s}}.$$
(4)

Here $a=(x_a,p_b)$ and $b=(x_b,p_b)$ refer to modes a and b, respectively. Furthermore, $K=1/(2\pi\sigma_0^2)^2$ is the normalization constant, σ_0^2 is the variance, and s is the squeezing factor

$$s = e^{2\zeta} . (5)$$

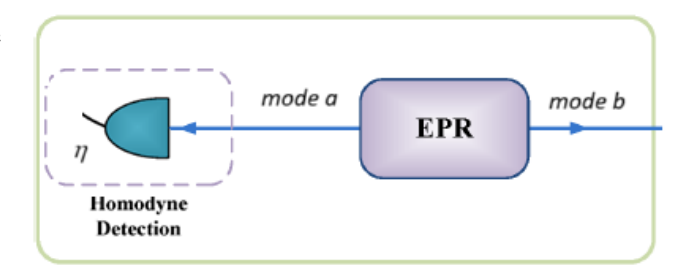
The effect of a measurement on one of the modes of a bipartite state can be described, in the Wigner function formalism, by the following general relation [8]

$$W_{\hat{\rho}_{cond,b}}(b) = \frac{\iint_{\mathbb{R}^2} W_{\hat{\Pi}_{x_0}}(a) W_{\hat{\rho}_{ab}}(a,b) da}{\iiint_{\mathbb{R}^4} W_{\hat{\Pi}_{x_0}}(a) W_{\hat{\rho}_{ab}}(a,b) da db}$$
(6)

In the equation above, $W_{\hat{\Pi}_{x_0}}$ is the phase-space representation of the measurement operator $\hat{\Pi}_{x_0}$ corresponding to the outcome x_0 . Our goal is to use the above integral to determine the result of both ideal and non-ideal homodyne detection on mode

a of the EPR state given in Eq. 4. This system is ilustrated in Fig. 1.

Figure 1: A two-mode squeezed vacuum state (EPR state) source sends mode a for Alice and mode b for Bob. By Alice performing a homodyne measurement on mode a, Bob's mode b collapse to a squeezed state for $\eta = 1$, where η is the efficiency of the homodyne detector.



In the ideal case, homodyne detection of the quadrature \hat{x} with outcome x_0 is described by the following POVM element [8, 9, 7].

$$\hat{\Pi}_{x_0} = |x_0\rangle \langle x_0|. \tag{7}$$

In the phase-space representation, the projector above corresponds to a Dirac delta distribution centered at the value x_0 [8, 9]:

$$W_{\hat{\Pi}_{x_0}}(a) = \frac{1}{4\pi\sigma_0^2} \delta(x_a - x_0). \tag{8}$$

By substituting the expression above together with Eq. 4 into Eq. 6, and performing the integration, we obtain:

the above integral to determine the result of both ideal and non-ideal homodyne detection on mode
$$W_{\hat{\rho}_{cond,b}}(b) = K'e^{-\frac{(x_0 - x_b)^2}{4\sigma_0^2 s^2} - \frac{(x_0 + x_b)^2}{4\sigma_0^2/s^2} + \left(1 - \tilde{\lambda}^2\right)\left[x_0^2 - Ap_b^2\right]}.$$
(9)





Here, the constants are defined as follows:

$$K' = \frac{A\sqrt{\pi}}{\pi\sigma_0\sqrt{1-\tilde{\lambda}^2}},\tag{10}$$

$$A = \frac{1}{4\sigma_0^2 s^2} + \frac{1}{4\sigma_0^2/s^2}, \tag{11}$$

$$A = \frac{1}{4\sigma_0^2 s^2} + \frac{1}{4\sigma_0^2/s^2}, \qquad (11)$$

$$B = \frac{1}{4\sigma_0^2/s^2} - \frac{1}{4\sigma_0^2 s^2}, \qquad (12)$$

and $2\tilde{\lambda} = B/A$.

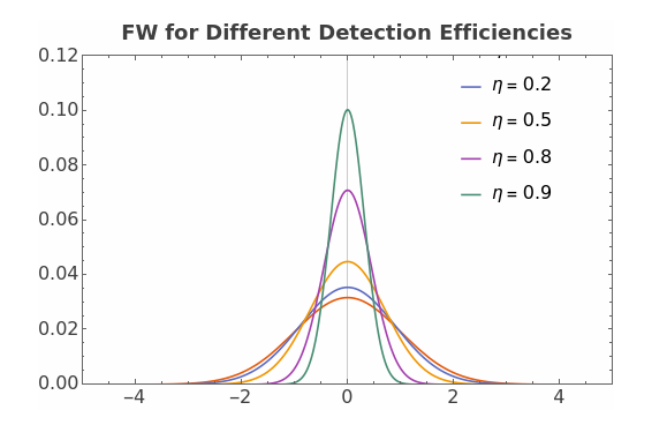
The expression above represents the Wigner function of an EPR state conditioned on an ideal homodyne measurement on mode a with outcome x_0 .

We now follow the same procedure, but consider a non-ideal homodyne measurement characterized by a finite detection efficiency η , which, the phase-space representation of the POVM [8]

$$W_{\hat{\Pi}_{\eta,x_0}}(a) = \frac{e^{\frac{(x_a - x_0)^2}{2\sigma_0^2(1-\eta)}}}{4\pi\sigma_0^2\sqrt{2\pi\sigma_0^2(1-\eta)}},$$
 (13)

depicted in Fig. 2

Figure 2: Comparison of the Wigner Function of the POVM for different quantum efficiencies η .



The equation above reduces to Eq.8 in the limit $\eta \to 1$, which corresponds to the ideal case. By

substituting this expression into Eq. 6, together with the EPR state, and evaluating the integral, we obtain the following Wigner function:

$$W_{\hat{\rho}_{cond,b}}^{\eta}(b) = \frac{e^{-\frac{(x_b - \bar{x}_b)^2}{2\sigma_x^2}} e^{-\frac{p_b^2}{2\sigma_p^2}}}{\sqrt{(2\pi\sigma_x^2)(2\pi\sigma_p^2)}}.$$
 (14)

The variances in position and momentum, after te measurement, are given, respectively, by

$$\sigma_x^2 = \frac{[2s + (1 - \eta)(s^2 + 1)]}{[(s^2 + 1) + 2(1 - \eta)s]}\sigma_0^2, \qquad (15)$$

$$\sigma_p^2 = \frac{(s^2 + 1)}{2s} \sigma_0^2 , \qquad (16)$$

and the mean displacement is expressed by

$$\bar{x}_b = -\frac{\sqrt{\eta}(s^2 - 1)}{[(s^2 + 1) + 2(1 - \eta)s]} x_0.$$
 (17)

Fig. 3 shows mode b Wigner function after mode a inefficient homodyne measurement. We see when EPR squeezing s increases, mode b x quadrature squeezes too.

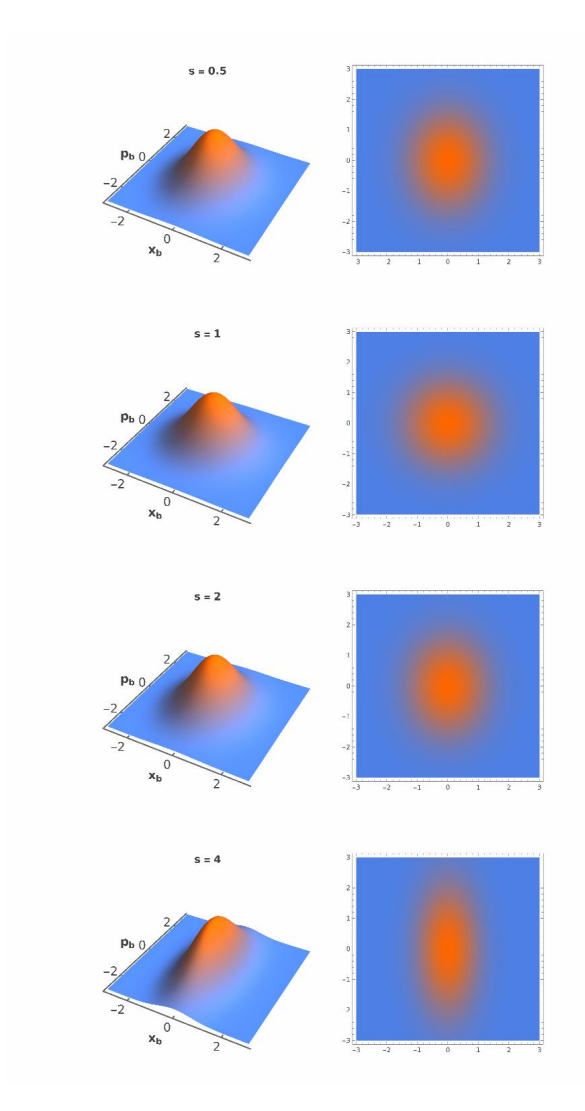
Fig. 4 shows mode b amplitude \bar{x}_b as function of inefficiency $(1 - \eta)$. We see inefficiency attenuate the amplitude value and EPR squeezing s increases the amplitude.

Note when s = 1 there is no EPR squeezing, mode b variances and x quadrature become $\sigma_x^2 = \sigma_p^2 =$ σ_0^2 and $\bar{x}_b=0$. This means measurement on mode a has no effect on mode b, as it should be, since zero squeezing is equivalent to separable state.





Figure 3: Wigner function of mode-b state, conditioned on the measurement in mode a, for different values of s.

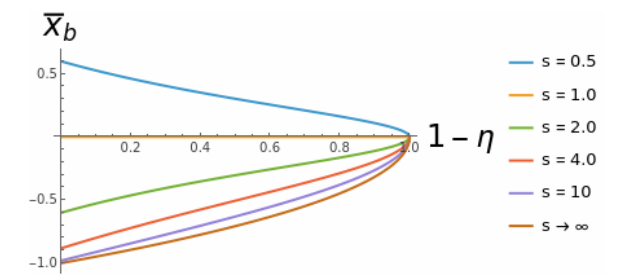


For the maximum efficiency ($\eta = 1$), mode b variances and x quadrature become σ_x^2 $\sigma_p^2 = \sigma_x^4$ and $\bar{x}_b = -x_0 (s^2 - 1)/(s^2 + 1)$. So, when variance p increases, variance x decreases, which is a squeezed state feature (we call this a perfect squeezed state).

4. Conclusion and outlook

analysis of how detector efficiency affects remote fects into comprehensive CV-QKD security anal-

Figure 4: Mode b quadrature amplitude $\bar{\mathbf{x}}_b$ as function of the inefficiency $1 - \eta$ for different values of squeezing parameter s.



state preparation in entangled systems. Using the Wigner function formalism, we derived the analytical form of the conditioned quantum state and demonstrated how homodyne detection inefficiencies on Alice's mode impact the prepared state on Bob's mode. Our results show that while homodyne measurement collapses Bob's mode into a squeezed state regardless of detector efficiency, inefficiencies attenuate the quadrature amplitude and degrade the squeezing. Importantly, when EPR squeezing is absent (s = 1), Bob's state remains unaffected by Alice's measurements, confirming the expected behavior for separable states.

These findings provide valuable insights for the practical implementation of CV-QKD protocols, where detector inefficiencies directly impact the amount of shared correlations. By quantifying how detection losses affect state preparation, our analysis establishes a foundation for developing more accurate security models that account for realistic detector performance. This work opens the In this work, we presented a theoretical and visual path toward incorporating detector inefficiency ef-



QUANTUM TECHNOLOGIES: The information revolution that will change the future





yses, enabling more precise estimation of achievable secret key rates.

Acknowlegement

This work has been fully funded by the project "Non-conventional Receivers for CV-QKD" supported by QuIIN - Quantum Industrial Innovation, EMBRAPII CIMATEC Competence Center in Quantum Technologies, with financial resources from the PPI IoT/Manufatura 4.0 of the MCTI grant number 053/2023, signed with EMBRAPII.

References

- [1] Vladyslav C. Usenko, Antonio Acín, Romain Alléaume, Ulrik L. Andersen, Eleni Diamanti, Tobias Gehring, Adnan A. E. Hajomer, Florian Kanitschar, Christoph Pacher, Stefano Pirandola, and Valerio Pruneri. Continuous-variable quantum communication.
- [2] Yichen Zhang, Yiming Bian, Zhengyu Li, Song Yu, and Hong Guo. Continuous-variable quantum key distribution system: Past, present, and future. <u>Applied Physics Reviews</u>, 11(1):011318, 2024.
- [3] F. Laudenbach, C. Pacher, C.-H. F. Fung, A. Poppe, M. Peev, B. Schrenk, M. Hentschel, P. Walther, and H. Hübel. Continuous-variable quantum key distribution with gaussian modulation—the theory of practical implementations. <u>Advanced Quantum Technologies</u>, 1(1):1800011, 2018.
- [4] Stefano Olivares. Introduction to generation, manipulation and characterization of optical quantum states. Physics Letters A, 418:127720, 2021.
- [5] Daniel Hogg, Dominic W Berry, and AI Lvovsky. Efficiencies of quantum optical detectors. Physical Review A, 90(5):053846, 2014.
- [6] Ulf Leonhardt. Measuring the quantum state of light, volume 22. Cambridge university press, 1997.
- [7] Alessandro Ferraro, Stefano Olivares, and Matteo GA Paris. Gaussian states in continuous variable quantum information. arXiv preprint quant-ph/0503237, 2005.
- [8] Olivier Morin. Non-Gaussian states and measurements for quantum information. PhD thesis, Université Pierre et Marie Curie-Paris VI, 2013.

- [9] Wolfgang P Schleich. Quantum optics in phase space. John Wiley & Sons, 2015.
- [10] E. Wigner. On the quantum correction for thermodynamic equilibrium. Phys. Rev., 40:749–759, Jun 1932.
- [11] Cosmas Zachos, David Fairlie, and Thomas Curtright.

 Quantum mechanics in phase space: an overview with selected papers. World Scientific, 2005.
- [12] Clemens Gneiting, Timo Fischer, and Klaus Hornberger. Quantum phase-space representation for curved configuration spaces. Physical Review A, 88(6):062117, 2013.